JOURNAL OF MAGNETIC RESONANCE **130,** 244–252 (1998)
ARTICLE NO. MN971306

On the Use of the Phase Memory Time T_2 for the Quantitative Characterization of the Rotational Motions of Proteins in Lipid Bilayer Systems

C. van der Struijf and Y. K. Levine[1]

Debye Institute, Buys Ballot Laboratory, P.O. Box 80.000, 3508 TA Utrecht, The Netherlands

Received April 28, 1997; revised October 16, 1997

Numerical simulations of the echo responses from a nitroxide label rigidly attached to a large protein undergoing ultraslow rotational motions in a lipid bilayer are presented. The echoes are formed by the application of Hahn, COSY, and 2D-ELDOR sequences utilizing both soft and hard microwave pulses. The simulations address the question of whether the echo responses elicited by these sequences are affected by restricted angular excursions of the long axis of the protein relative to the normal to the bilayer plane. The results indicate that all three pulse sequences yield the same quantitative motional information regardless of the nature of the microwave pulses and there is no theoretical reason for preferring one sequence above the others.

INTRODUCTION

The rotational motions of a large protein molecule embedded in a lipid bilayer system may be studied using electron-spin-echo (ESE) techniques. To this end the protein is labeled covalently with a nitroxide spin label. If the nitroxide spin label is rigidly attached to the protein, the ESE experiments effectively monitor the rigid body motions of the protein (*1*). These are expected to take place on the microsecond time scale. Commonly, membrane proteins are assumed to be anchored rigidly in the lipid bilayer matrix and undergo rotational motions about an axis perpendicular to the bilayer plane.

We have previously reported a study of the rotational motions of the intrinsic membrane protein Ca-ATPase (*1*) using Hahn echo experiments (*2–4*). The dispersion of phase memory time T_2 obtained from the decay of the echo amplitude with the interpulse time provided quantitative information about the motional rates of the protein and its aggregates in the bilayer system. The rotational rates were obtained by simulating the experiments in the time domain by solving the Bloch equations for the stochastic spin Hamiltonian on making use of stochastic trajectories for the orientational behavior of the spin-labeled protein. The simulations indicated that while an axial motion of the protein accounted for the observed echo responses, an additional motion of the axis of rotation relative to the bilayer plane could not be ruled out.

Here we will address the question as to whether the echo responses elicited by any of the common pulse sequences monitoring the phase memory time T_2 of nitroxides are affected by a restricted motion of the protein axis relative to the bilayer normal. To this end we shall consider correlation spectroscopy (COSY) (*2, 5*) and two-dimensional electron double resonance (2D-ELDOR) (*2–4, 6–8*) as well as the Hahn sequence. The echo responses from nitroxide labels undergoing ultraslow rotational motions following the application of these echo sequences were calculated numerically in the time domain. The simulations made use of trajectories of the stochastic orientation of the nitroxide label during the course of the experiment. The advantage of this approach is that the trajectories corresponding to different prescriptions of rotational motion can be generated in a straightforward way, which is moreover independent of the calculation of the evolution of the magnetization in time. In particular we investigated whether it is possible to distinguish between two simple models for the motion of a nitroxide label rigidly attached to a large protein embedded in a lipid bilayer. In the first place the proteins will be assumed to undergo a purely axial motion about the normal to the membrane. In the second place the axis itself will be allowed to undergo restricted orientational motions.

The simulations indicate that rotational motions affect the echo responses of all three pulse sequences in an analogous manner, regardless of the nature of the microwave pulses. There is thus no theoretical reason for preferring one sequence above the others.

THEORY

Hahn, COSY, and 2D-ELDOR Pulse Sequences

The pulse sequence for the Hahn echo

$$\left(\frac{\pi}{2}\right)_x - \tau - (\pi)_x - \text{acquire}_y \qquad [1]$$

[1] To whom correspondence should be addressed.

1090-7807/98 $25.00

is analogous to the COSY sequence which utilizes a second $\pi/2$ pulse instead of a π pulse:

$$\left(\frac{\pi}{2}\right)_x - \tau - \left(\frac{\pi}{2}\right)_x - \text{acquire}_y. \quad [2]$$

The 2D-ELDOR method rests on the application of a sequence of three $\pi/2$ pulses, separated by two interpulse times τ and T:

$$\left(\frac{\pi}{2}\right)_x - \tau - \left(\frac{\pi}{2}\right)_x - T - \left(\frac{\pi}{2}\right)_x - \text{acquire}_y. \quad [3]$$

Here the interpulse time τ is varied while T is kept constant at a predetermined value. We shall here consider only the application of these pulse sequences to oriented bilayer samples and employ the following phase cycling schemes (*2, 9*) in the simulations of the echo response.

For the Hahn pulse sequence

$$\begin{aligned}
&\text{step1:} \quad \left(\frac{\pi}{2}\right)_x - \tau - (\pi)_x - \text{acquire}_{x+y}\\
&\text{step2:} \quad x - \tau - y - \text{acquire}_{x+y}\\
&\text{step3:} \quad x - \tau - -x - \text{acquire}_{x+y}\\
&\text{step4:} \quad x - \tau - -y - \text{acquire}_{x+y}, \quad [4]
\end{aligned}$$

where acquire_{x+y} indicates that the in-phase and the out-of-phase components of the time response are measured. Knowledge of both these components is necessary for the Fourier transformation of the signal into the frequency domain. The total echo form E for each component is obtained as

$$E = \text{step1} - \text{step2} + \text{step3} - \text{step4}. \quad [5]$$

For the COSY experiment we shall exploit the following four-step phase cycle scheme:

$$\begin{aligned}
&\text{step1:} \quad \left(\frac{\pi}{2}\right)_x - \tau - \left(\frac{\pi}{2}\right)_x - \text{acquire}_{x+y}\\
&\text{step2:} \quad y - \tau - y - \text{acquire}_{x+y}\\
&\text{step3:} \quad -x - \tau - -x - \text{acquire}_{x+y}\\
&\text{step4:} \quad -y - \tau - -y - \text{acquire}_{x+y}. \quad [6]
\end{aligned}$$

The total echo forms for the in-phase and out-of-phase components are now given by

$$\begin{aligned}
E_{\text{in-phase}} &= \text{step1}_x - \text{step2}_y - \text{step3}_x + \text{step4}_y\\
E_{\text{out-phase}} &= \text{step1}_y + \text{step2}_x - \text{step3}_y - \text{step4}_x. \quad [7]
\end{aligned}$$

A more complex phase cycling procedure is needed for the 2D-ELDOR sequence. The scheme consists of the following eight phase cycling steps:

$$\begin{aligned}
&\text{step1:} \quad \left(\frac{\pi}{2}\right)_x - \tau - \left(\frac{\pi}{2}\right)_x - T - \left(\frac{\pi}{2}\right)_x - \text{acquire}_{x+y}\\
&\text{step2:} \quad y - \tau - y - T - y - \text{acquire}_{x+y}\\
&\text{step3:} \quad x - \tau - x - T - -x - \text{acquire}_{x+y}\\
&\text{step4:} \quad y - \tau - y - T - -y - \text{acquire}_{x+y}\\
&\text{step5:} \quad x - \tau - -x - T - -x - \text{acquire}_{x+y}\\
&\text{step6:} \quad y - \tau - -y - T - -y - \text{acquire}_{x+y}\\
&\text{step7:} \quad x - \tau - -x - T - x - \text{acquire}_{x+y}\\
&\text{step8:} \quad y - \tau - -y - T - y - \text{acquire}_{x+y}. \quad [8]
\end{aligned}$$

The total echo forms E for the in-phase and out-of-phase components are given in this case by

$$\begin{aligned}
E_{\text{in-phase}} &= \text{step1}_x - \text{step2}_y - \text{step3}_x + \text{step4}_y\\
&\quad + \text{step5}_x - \text{step6}_y - \text{step7}_x + \text{step8}_y\\
E_{\text{out-phase}} &= \text{step1}_y + \text{step2}_x - \text{step3}_y - \text{step4}_x\\
&\quad + \text{step5}_y + \text{step6}_x - \text{step7}_y - \text{step8}_x. \quad [9]
\end{aligned}$$

Hard and Soft Pulses

In applying the sequences of pulses one must bear in mind that the strength of the microwave field $\boldsymbol{B}_1$ influences the formation of the echo. Pulses utilizing high fields, the so-called hard pulses, contain sufficient frequency components to cover the entire CW-ESR absorption spectrum and thus rotate the entire magnetization uniformly by $\pi/2$ or π. This is true in the vast majority of NMR experiments (*10, 11*). In this case, the echo shape is simply the Fourier transform of the absorption spectrum as can be seen in Fig. 1. A typical Hahn echo response with an interpulse time $\tau = 100$ ns together with the corresponding frequency-domain response obtained by Fourier transformation is shown. The magnetic field is given as an offset relative to the center of the spectrum at 3373 G.

It is unfortunately not always feasible to obtain hard pulses for nitroxide labels in oriented lipid bilayer systems using current ESR instrumentation. In most circumstances the microwave field generated is too weak to cover the broad CW absorption spectrum. For this reason we shall also consider the case of soft, or selective, pulses which irradiate only a portion of the spectrum. With these pulses the on-resonance magnetization is rotated by the desired amount and the angle of rotation decreases rapidly on moving away from resonance. Echoes from sequences utilizing soft pulses are consequently acquired across the spectrum at different positions of the applied Zeeman field.

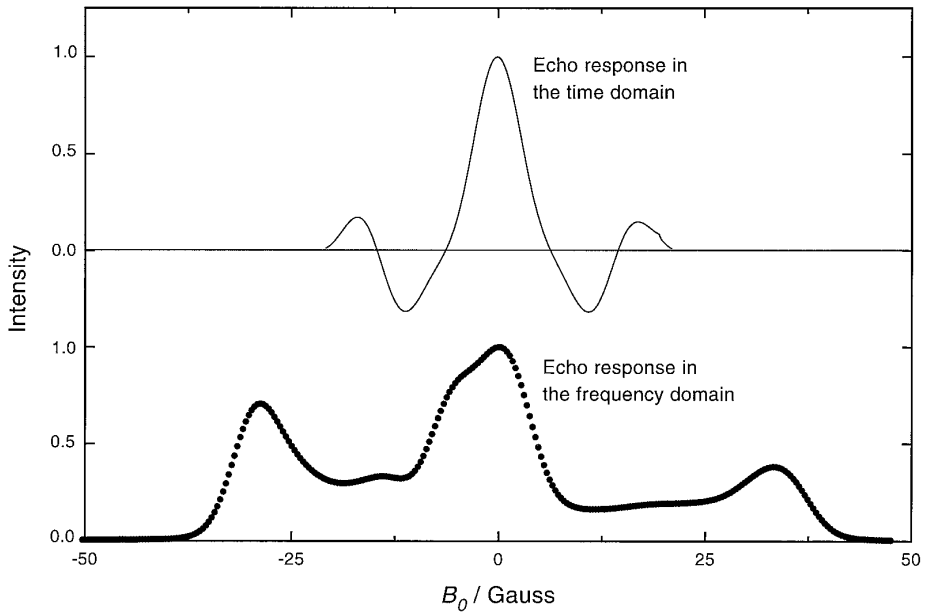

FIG. 1. The echo responses to a Hahn sequence utilizing hard pulses in the time and frequency domains. Both spectra are normalized to 1 at their respective maxima.

COMPUTATION OF THE ECHO RESPONSE

General Approach

The spin Hamiltonian of the nitroxide labels is taken to be (*12*)

$$H = B_0 \cdot \mathbf{g}(\Omega) \cdot S_z + I \cdot \mathbf{A}(\Omega) \cdot S_z, \qquad [10]$$

where we have neglected the contribution from the nuclear Zeeman interactions. While these interactions are expected to modulate the echo response to sequences using hard pulses (*13*), they are of subsidiary importance for our present purpose.

The **A** and the **g** tensors in the nitroxide frame were taken to be

$$\mathbf{A} = \begin{pmatrix} 5.6 & 0 & 0 \\ 0 & 5.3 & 0 \\ 0 & 0 & 34.0 \end{pmatrix} \qquad [11]$$

$$\mathbf{g} = \begin{pmatrix} 2.0096 & 0 & 0 \\ 0 & 2.0061 & 0 \\ 0 & 0 & 2.0021 \end{pmatrix}. \qquad [12]$$

Here we shall focus on differences in the echo responses arising from different modes of motions of the nitroxide labels. In essence, we shall concentrate on the behavior of the autopeaks in the Fourier spectra, i.e., those peaks occurring at the center of the Fourier spectra, obtained with sequences using hard pulses.

The evolution of the magnetization is calculated on dividing the pulse sequence into time steps whose lengths are small compared to the total length of the sequence following the procedure described previously in (*1, 14*) and a program listing can be obtained from the authors. The algorithm rests on the idea that the orientation of the nitroxide fully determines its resonance frequency as is appropriate for rotational motions on the microsecond time scale. The phase cycling steps, see Eqs. [4]–[9], are implemented in a straightforward way, by repeating the calculation for each step along the identical trajectory of orientations. Considerable savings in cpu time can be realized by a judicious arrangement of the phase cycling steps, so that only changes need to be evaluated at any stage of the procedure.

The most important ingredient of the algorithm is the calculation of the effect of the finite width of the microwave pulses. Each pulse is considered to consist of a series of small ideal pulses. An ideal pulse rotates the magnetization of every spin packet in the ensemble instantaneously around the direction of $\boldsymbol{B}_1$ irrespective of its resonance frequency. In the time between the pulses, the individual spin packets precess around the z axis for a time corresponding to the time grid used in the calculation. The precession frequency is updated, corresponding to the (new) orientation of the probe, before the application of the next ideal pulse. This ideal pulse–precess cycle is repeated during the application of the real microwave pulse. In the practical implementation of the algorithm, a $\pi/2$ pulse of strength 2.2 G (t_{90} = 40 ns) is divided into 40 ideal pulses, each of which rotates the magnetization by 2.25° about the x axis of the rotating frame. The magnetization of the individual spin packets precesses about the z axis for 1 ns. The differences in precession

frequencies of the spin packets cause the loss of mutual phase coherence and consequently the net magnetization in the $x-y$ plane quickly decays to zero. This is, however, a reversible process. An irreversible loss of phase coherence is caused by the stochastic changes in resonance frequencies due to probe motion. The nonmotional relaxation mechanisms are considered to cause a simple exponential damping of the different components of the magnetization.

The echo responses to sequences using soft pulses are calculated across the CW-ESR absorption spectrum, by simply changing the value of $\boldsymbol{B}_0$. The calculation is repeated for different times between the first and second pulses. The echo response along the positive y axis is evaluated and the signal is integrated over a time window of width 200 ns centered at the position of the echo maximum. The integrated intensity is subsequently plotted as a function of field position and interpulse time.

The echo responses evaluated with sequences of hard pulses are furthermore Fourier transformed into the frequency domain. The first dimension of the Fourier spectra reflects the variation of the interpulse time, the time between the first and second pulse. The second dimension is determined by the time following the last pulse of the sequence. The response is followed for a time τ_2 following the echo maximum. The Fourier transformation requires knowledge of both the out-of-phase signal (the response along the positive y axis) and the in-phase signal evaluated along the positive x axis. The Fourier spectra were calculated by using algorithms from ''Numerical Recipes'' (*15*).

Motional Models

We shall here assume that the nitroxide labels undergo small step diffusion about their body-fixed principal axes. The trajectory of molecular orientations is obtained by allowing the label to undergo stochastic jumps of maximal size $\Delta\theta_\eta$, where η denotes the x, y, or z axis. Note that isotropic motion results when $\Delta\theta_\eta$ is identical for all three axes. Any molecular reorientation involves rotations about all three axes. The order of the rotations and the size of the angular excursions are chosen at random. The three Euler angles α, β, and γ are evaluated using the standard rotational transformation from the molecular to the laboratory frame (*16*).

An added advantage of this approach is that the monoexponential decay time of the correlation functions $G_{mn}(t) = \langle D^2_{mn}(\Omega_0) D^{*2}_{mn}(\Omega_t)\rangle$, calculated along the trajectory scales with $(\Delta\theta_\eta)^{-2}$. The algorithm may be checked by showing that all the calculated correlation functions $G_{mn}(t)$ are characterized by the same decay time within the statistical uncertainties as expected for an isotropic rotational motion.

We shall here consider only nitroxide molecules undergoing rotations with a maximal step size of $\Delta\theta = 0.25°$ per nanosecond about each of their body-fixed axes. This corresponds to a rotational correlation time of 200 μs appropriate for the motions of Ca-ATPase in lipid bilayers (*1*).

In order to describe restricted rotations, the long axis of the protein is subjected to the action of an orienting potential. This potential is infinite for the case of axial rotations, and is zero for a uniform, isotropic tumbling of the axis. For the sake of simplicity we shall here implement a particular form of orienting potential, commonly known as the wobble-in-cone model (*14*). Here, the z axis moves freely within a cone of half-angle β_0 and with infinite potential walls:

$$U(\beta) = 0 \quad \text{for } 0° \le \beta \le \beta_0$$
$$U(\beta) = \infty \quad \text{for } \beta_0 < \beta \le 180°. \qquad [13]$$

In all the simulations we have taken the cone half-angle β_0 to be 30°. We shall furthermore focus our attention to two limiting cases determined by the orientation of the bilayer normal defining the axis of the cone, $\boldsymbol{n}$, with respect to the static magnetic field $\boldsymbol{B}_0$. In the first case, $\boldsymbol{n}$ is parallel to $\boldsymbol{B}_0$, so that the molecular and laboratory frames coincide. In the second case $\boldsymbol{n}$ is perpendicular to $\boldsymbol{B}_0$. The echo response in the presence of motion is first calculated in the molecule frame and subsequently transformed to the laboratory frame. The rotational transformation required leaves us with a choice as to the orientation of the cone axis $\boldsymbol{n}$ in the xy plane. We have, however, found identical echo responses for cones lying in different positions in that plane. This is consistent with the observation that the precession frequencies of the nitroxide are independent of the Euler angle α which here defines the orientation of the cone axis relative to the x axis (*14, 17*).

Computational Details

The echo responses were calculated for an ensemble of 15,000 nitroxide molecules. The initial orientations can be chosen at random within a cone when appropriate.

The $\pi/2$ hard pulses were taken to be 5 ns long, corresponding to experimental situations (*18*), and were divided into time slices of 0.25 ns for the computation of the echo response. This choice is a useful compromise between cpu time and reliability of the computed echo response. In fact, no changes in the echo responses were observed on choosing a finer mesh for the calculations. The evolution of the magnetization between the pulses was sampled at intervals of 1–2.5 ns. The echo response was computed at 1-ns steps following the last pulse of the sequence and was monitored for 128 ns after reaching its maximum. The interpulse time τ was increased in steps of 5 ns along the range of 100–740 ns, thus yielding 128 points for the Fourier transformation.

The length of the $\pi/2$ soft pulse was chosen to be 40 ns as in (*1*), and it was divided into intervals of 2 ns in the computations. The echo response was integrated in a time window of 200 ns centered around the echo maximum. The echo response in the frequency domain was subsequently obtained with a 2D Fourier transformation of 128 $\times$ 128 points. In this way a good signal-to-noise ratio was obtained

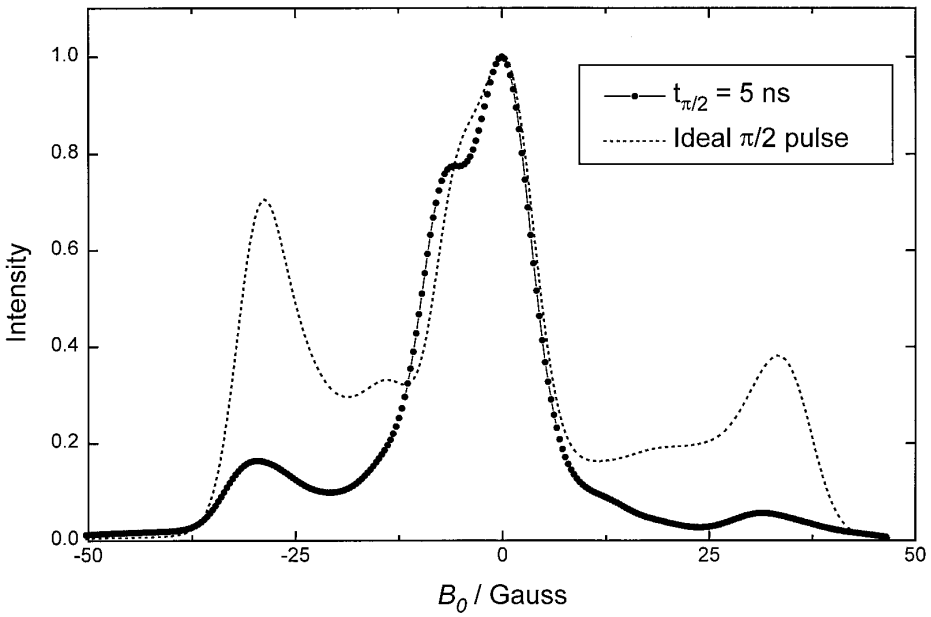

FIG. 2. The influence of the length of the $\pi/2$ pulse of a Hahn pulse sequence. The maxima of both spectra are normalized to 1.

and moreover, no significant improvement was obtained by sampling the echo response for times of 256 ns or even longer. Note that for the three-pulse 2D-ELDOR sequence the interpulse time T between the second and third pulses was kept fixed at 300 ns, as used experimentally by Freed and co-workers in studies of the behavior of CSL in lipid bilayers (*18*).

Finally, an additional Gaussian broadening of 2.5 G was superimposed on the calculated spectra to account for the effects of unresolved hyperfine couplings between the electron and the surrounding proton spins (*19*).

The computation of the echo response of a single pulse sequence required around 2 min cpu time on a SUN10 workstation. A total computational effort of 30 h cpu time was needed on average to generate phase-cycled responses with a sufficient statistical reliability.

RESULTS

We shall here consider the echo response elicited by the three pulse sequences described above from a model system of a nitroxide label rigidly bound to protein molecules such as Ca-ATPase in lipid bilayers (*1*). The nitroxide label is taken to be attached to the protein such that its y axis coincides with the z axis of the protein. In this orientation the spin Hamiltonian exhibits an optimal senitivity to the rotational motions of the protein. Two possible modes of motions within the cone are considered below. The first is *axial rotation*, whereby the protein reorients about its z axis, with the axis itself stationary and aligned along the normal to the bilayer surface. In the second, *motion in a cone*, the protein undergoes rotation about its z axis, and the axis itself is allowed to tumble freely within the confines of a cone of half-angle of 30°. The echo responses were evaluated for two limiting cases of the magnetic field $\boldsymbol{B}_0$ applied along and perpendicular to the bilayer normal, which coincides with the axis of the cone, $\boldsymbol{n}$.

The first question to be addressed is whether $\pi/2$ pulses of 5-ns width satisfy the criterion for hard pulses, namely that they are short enough to completely cover the CW-ESR absorption spectrum. This was found to be the case for the COSY and 2D-ELDOR sequences, but interestingly not for the Hahn experiment. The reason for this appears to be the use of a π pulse, 10 ns long, in the latter sequence. This is illustrated in Fig. 2, where echo responses calculated with pulses of finite length, $\pi/2$ pulse of 5 ns, and ideal δ pulses are shown. It can be easily seen that only the ideal pulses rotate the entire CW-ESR spectrum. For this reason we have chosen to use ideal δ pulses for the calculations of the echo responses elicited by the Hahn pulse sequences.

Hard Pulses

The Fourier spectra of the Hahn echo responses with $\boldsymbol{B}_0$ perpendicular to the cone axis for the axial and conic modes of motion are shown in Fig. 3. The overall shape of the autopeaks in the given Fourier spectra bear a strong resemblance to the experimental spectra reported by Freed and coworkers (*3, 18*). The spectra show a marked hyperfine structure, which is almost identical in both cases. The similarity is evident in Fig. 5 which shows a cross section of the spectra through the $\omega = 0$ plane. In marked contrast, featureless Fourier spectra are found when $\boldsymbol{B}_0$ is aligned parallel to $\boldsymbol{n}$, Fig. 4. However, now the spectrum for the motion in a cone is

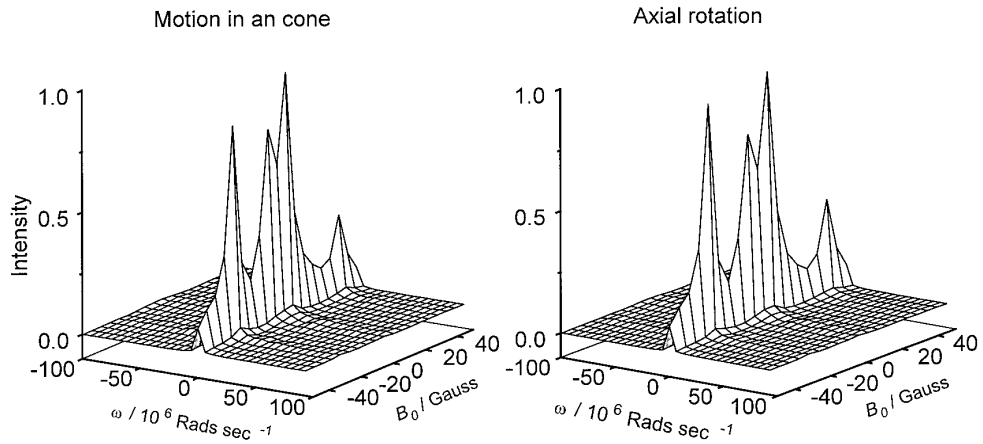

FIG. 3. Simulated Fourier spectra of the echo responses to Hahn sequences using hard pulses with the magnetic field $\boldsymbol{B}_0$ perpendicular to the bilayer normal/cone axis $\boldsymbol{n}$.

substantially narrower than that for the axial rotation as can be seen from the cross section at $\omega = 0$, Fig. 5.

The Fourier spectra computed for the COSY and 2D-ELDOR pulse sequences are similar to those obtained with the Hahn sequence and moreover exhibit the same differences between the two modes of motion. The corresponding cross sections at $\omega = 0$ are shown in Fig. 5 for the two orientations of the static field $\boldsymbol{B}_0$ relative to $\boldsymbol{n}$.

The results reported above suggest the following protocol for the characterization of the modes of motion of the nitroxide label from experimental echo responses elicited by sequences utilizing hard pulses. In the first place, the Fourier spectra obtained with $\boldsymbol{B}_0$ oriented perpendicular to the bilayer normal and the cone axis are first analyzed using a particular motional model. The parameters extracted from the fitting procedure are subsequently used to simulate the spectra obtained with $\boldsymbol{B}_0$ parallel to $\boldsymbol{n}$. The discrepancies between the simulations and experimental spectra are now a measure of the fidelity of the model.

This prescription raises two experimental problems. In the first place, the direction of the cone axis is not known a priori, and needs to be determined for the system at hand. This implies that the Fourier spectra or simply the CW-ESR spectra must be recorded as a function of the orientation of $\boldsymbol{B}_0$ relative to the plane of the bilayer. In the second place, our findings indicate that it is imperative to work with macroscopically aligned membrane systems. The experimentally convenient isotropic vesicle systems cannot be used to extract quantitative information about the motion of the nitroxide label, as they yield a superposition of spectra from different orientations relative to the applied static field.

The protocol suggested here for extracting quantitative information about the rotational motion of nitroxide labels on the microsecond time scale is in fact analogous to that commonly used in studies of the motions of nitroxide labels in lipid bilayer on the nanosecond time scale. The latter studies rest on the effect of rotational motion on the lineshape of the CW-ESR spectrum. In particular the analysis

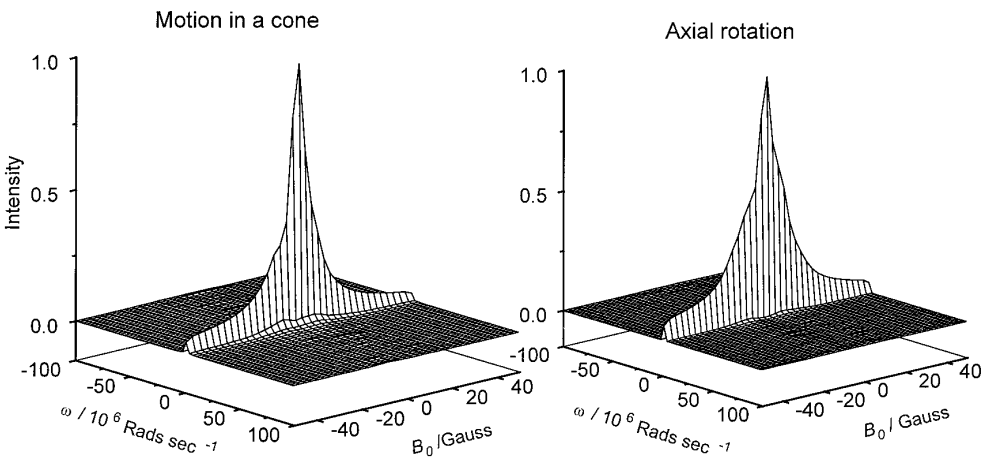

FIG. 4. Simulated Fourier spectra of the echo responses to Hahn sequences using hard pulses with the magnetic field $\boldsymbol{B}_0$ parallel to $\boldsymbol{n}$.

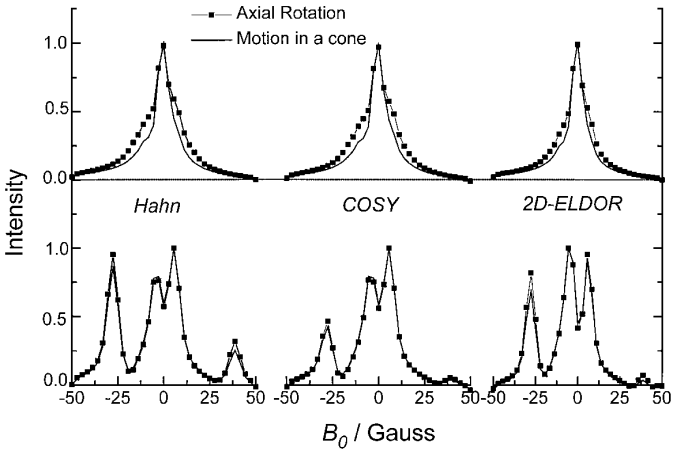

FIG. 5. Cross sections at $\omega = 0$ of the Fourier spectra of the echo responses of the Hahn, COSY, and 2D-ELDOR sequences utilizing hard pulses. (Top) $\boldsymbol{B}_0$ parallel to $\boldsymbol{n}$; (bottom) $\boldsymbol{B}_0$ perpendicular to $\boldsymbol{n}$.

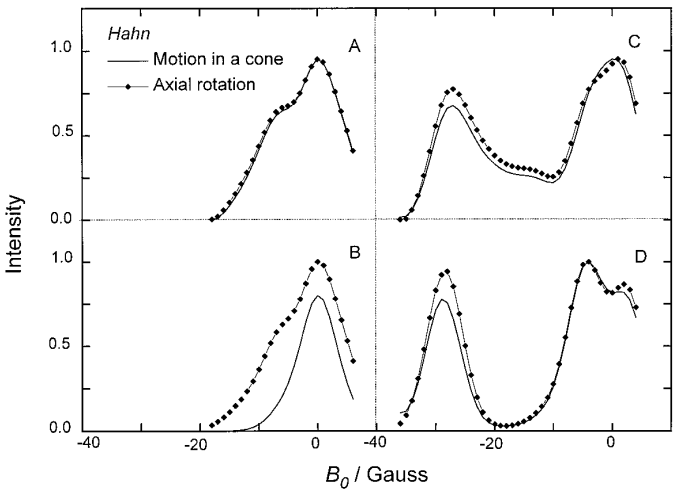

FIG. 7. Time slices of the Hahn soft pulse simulations. (A) $\boldsymbol{B}_0$ parallel to $\boldsymbol{n}$ and $\tau = 100$ ns; (B) as A but with $\tau = 500$ ns; (C) $\boldsymbol{B}_0$ perpendicular to $\boldsymbol{n}$ at $\tau = 100$ ns; (D) as C but at $\tau = 500$ ns. The echo intensities are normalized relative to those given by axial motion.

makes use of the variation of the hyperfine structure on changing the orientation of $\boldsymbol{B}_0$ relative to the bilayer plane. The CW-ESR spectra from macroscopically isotropic samples exhibit few structural features and their quantitative analysis is consequently often open to question (*20, 21*).

Soft Pulses

Soft microwave pulses rotate only a small portion of the CW-ESR spectrum by the desired amount, $\pi/2$ or π. It is thus usual to apply sequences of soft pulses at different positions of the magnetic field $\boldsymbol{B}_0$ within the CW-ESR spectrum and to monitor the echo intensity in the time domain as a function of the interpulse time τ. Thus in contrast to the case of sequences of hard pulses, the echo responses are computed in the time domain only as a function of τ and $\boldsymbol{B}_0$. It is important to note here that we were unable to obtain echo responses with a sufficient signal-to-noise ratio on the high-field side of the CW absorption spectrum using an acceptable computational effort. This reflects the low echo responses observed experimentally (*1, 14*). We shall therefore restrict our attention to the low-field and central peak spectral regions.

Typical echo responses of the COSY pulse sequence evaluated using the axial and conic motional modes are shown in Fig. 6. Here $\boldsymbol{B}_0$ is applied in a direction perpendicular to the cone axis. Almost identical responses are elicited by the Hahn and 2D-ELDOR sequences.

The differences between the two modes of motion of the nitroxide label should now be reflected not only in the rates of the echo intensity decay but also in their dependence on the magnetic field position. The variations of the echo intensity resulting from the application of a Hahn sequence with interpulse times of 100 and 500 ns are shown in Fig. 7 for

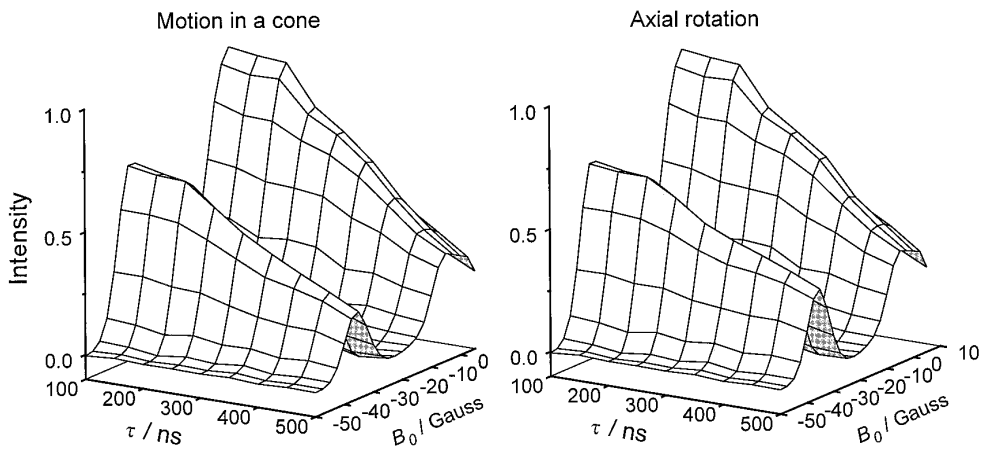

FIG. 6. Two-dimensional plot of the temporal and magnetic field dependence of the echo intensity simulated for the COSY sequence utilizing soft pulses. The intensities have been normalized to 1 at their maxima for $\tau = 100$ ns and $\boldsymbol{B}_0$ is perpendicular to the bilayer normal/cone axis $\boldsymbol{n}$.

the two motional modes with $\boldsymbol{B}_0$ parallel and perpendicular to $\boldsymbol{n}$. It can be clearly seen that axial rotation affects the echo decay rates virtually uniformly over the CW-ESR spectra obtained with with $\boldsymbol{B}_0$ parallel to $\boldsymbol{n}$. However, it produces smaller relaxation effects than the motion in a cone. Nonetheless, an enhancement of the echo decay rates can be obtained by implementing faster rates of axial motion. Interestingly, both modes of motion have a similar effect on the echo response when $\boldsymbol{B}_0$ is applied in a direction perpendicular to the cone axis, Fig. 7. Nevertheless, we find that the ratio of the echo decay rates at the peak maxima varies on increasing the interpulse time. The same behavior is exhibited by the echo responses calculated for the COSY and 2D-ELDOR pulse sequences, Figs. 8 and 9. It thus appears that any of the three pulse sequences may be used equally well for characterizing the modes of motion of the nitroxide labels.

The findings reported here indicate that the strategy to be followed in extracting quantitative information about the motional mode of the labels is analogous to that described above for the hard pulse sequences. Importantly, our findings explain why the echo decays observed from macroscopically isotropic samples of lipid bilayers containing nitroxide-labeled Ca-ATPase (*1*) can be analyzed using different models for rotational motion.

CONCLUSIONS

We have here calculated numerically the echo responses from nitroxide labels undergoing ultraslow rotational motions following the application of Hahn, COSY, and 2D-ELDOR sequences utilizing both soft and hard microwave pulses. The calculations were carried out in the time domain and made use of trajectories of the stochastic orientation of the nitroxide label during the course of the experiment. The advantage of this approach is that the trajectories corresponding to different prescriptions of rotational motion can be generated in a straightforward way, which is moreover independent of the calculation of the evolution of the magnetization in time. The computational effort involved in our approach is modest compared to that required for computations in the frequency domain (*22*), and hence can be extended to deal with more sophisticated pulse sequences and even macroscopically isotropic samples.

The pulse sequences considered here monitor the phase memory time T_2 of the nitroxide labels and our simulations were concerned with the way rotational motion affects this relaxation mechanism. In particular we investigated whether it is possible to use these sequences to distinguish between two simple models for the motion of a nitroxide label rigidly attached to a large protein embedded in a lipid bilayer. The proteins were either aligned perfectly along the normal to the bilayer plane or confined to a cone fixed rigidly in the bilayer. Thus the static magnetic field $\boldsymbol{B}_0$ can be applied in different directions relative to their long axis. We mimicked experimental situations by computing the echo responses to pulse sequences using both hard and soft microwave pulses. The results show that rotational motions have the same effect on the responses elicited by all three pulse sequences regardless of the nature of the microwave pulses. Thus there is no theoretical reason for preferring one sequence above the others.

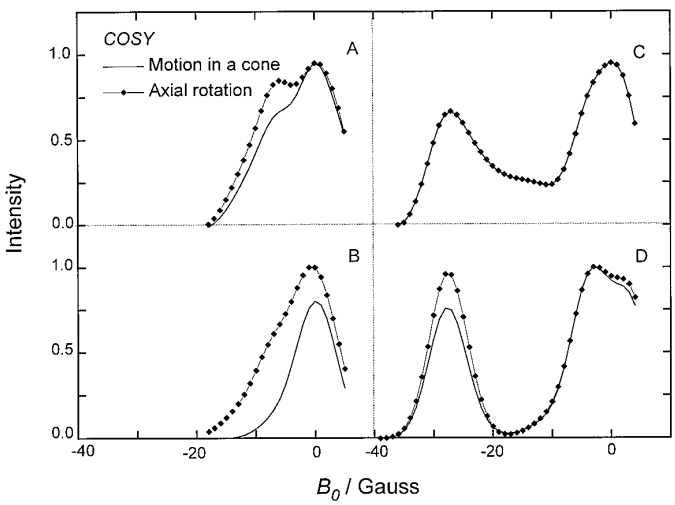

FIG. 8. Time slices of the COSY soft pulse simulations. (A) $\boldsymbol{B}_0$ parallel to $\boldsymbol{n}$ and $\tau = 100$ ns; (B) as A but with $\tau = 500$ ns; (C) $\boldsymbol{B}_0$ perpendicular to $\boldsymbol{n}$ at $\tau = 100$ ns; (D) as C but at $\tau = 500$ ns. The echo intensities are normalized relative to those given by axial motion.

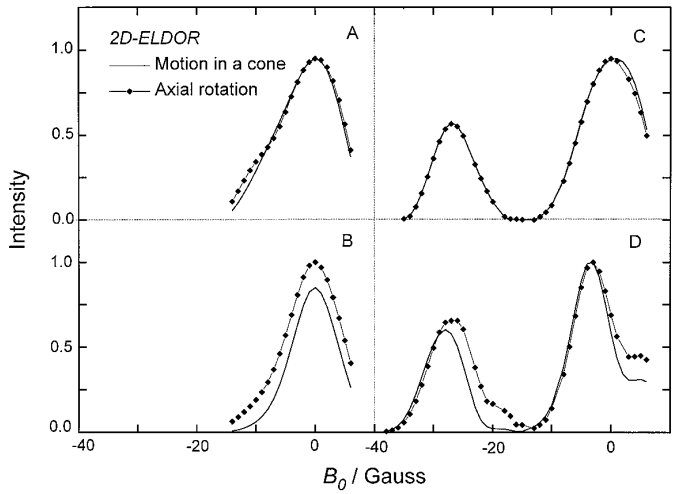

FIG. 9. Time slices of the 2D-ELDOR soft pulse simulations. (A) $\boldsymbol{B}_0$ parallel to $\boldsymbol{n}$ and $\tau = 100$ ns; (B) as A but with $\tau = 500$ ns; (C) $\boldsymbol{B}_0$ perpendicular to $\boldsymbol{n}$ at $\tau = 100$ ns; (D) as C but at $\tau = 500$ ns. The echo intensities are normalized relative to those given by axial motion.

REFERENCES

1. C. van der Struijf, T. Ph. Pelupessy, E. E. van Faassen, and Y. K. Levine, *J. Magn. Reson. B* **111,** 158 (1996).
2. D. Gamliel and J. H. Freed, *J. Magn. Reson.* **89,** 60 (1990).

3. G. L. Millhauser, Ph.D. thesis, Cornell University (1986).
4. G. L. Millhauser and J. H. Freed, *J. Chem. Phys.* **81,** 37 (1984).
5. R. Song, Y. C. Zhong, C. J. Noble, J. R. Pilbrow, and D. R. Hutton, *Chem. Phys. Lett.* **247,** 477 (1996).
6. J. Gorcester, G. L. Millhauser, and J. H. Freed, *in* ''Advanced EPR'' (A. J. Hoff, Ed.), p. 453, Elsevier, Amsterdam (1989).
7. B. R. Patyal, R. H. Crepeau, D. Gamliel, and J. H. Freed, *Chem. Phys. Lett.* **175,** 453 (1990).
8. A. Schweiger, *Angew. Chem. Int. Ed. Engl.* **30,** 265 (1991).
9. H. Eviatar, Y. K. Levine, and D. I. Hoult, *J. Magn. Reson. A* **117,** 41 (1995).
10. A. E. Derome, ''Modern NMR Techniques for Chemistry Research,'' Pergamon Press, Oxford (1993).
11. R. R. Ernst, G. Bodenhausen, and A. Wokaun, ''Principles of Nuclear Magnetic Resonance in One and Two Dimensions,'' Oxford Univ. Press, New York (1987).
12. C. P. Slichter, ''Principles of Magnetic Resonance,'' Springer-Verlag, Berlin/New York (1990).
13. W. B. Mims, *Phys. Rev. B* **5,** 2409 (1972); **6,** 3543 (1972).
14. C. Van der Struijf, Ph.D. thesis, Utrecht University (1997).
15. W. H. Press, W. T. Vetterling, S. A. Teukolsky, and B. P. Flannery, ''Numerical Recipes,'' Cambridge Univ. Press, Cambridge (1992).
16. M. P. Allen and D. J. Tildesley, ''Computer Simulations of Liquids,'' Clarendon Press, Oxford (1987).
17. L. J. Libertini and O. H. Griffith, *J. Chem. Phys.* **53,** 1359 (1970).
18. R. H. Crepeau, S. Saxena, S. Lee, B. Patyal, and J. H. Freed, *Biophys. J.* **66,** 1489 (1994).
19. G. R. Luckhurst and A. Sanson, *Mol. Phys.* **24,** 1297 (1972).
20. M. Ge-M and J. H. Freed, *Biophys. J.* **65,** 2106 (1993).
21. E. Meirovitch, A. Nayeem, and J. H. Freed, *J. Phys. Chem.* **88,** 3454 (1984).
22. S. Lee, B. R. Patyal, and J. H. Freed, *J. Chem. Phys.* **98,** 3665 (1993).